Multiobjective Optimization Applied to Robust $\mathcal{H}_2/\mathcal{H}_\infty$ State-feedback Control Synthesis

Eduardo N. Gonçalves, Reinaldo M. Palhares, and Ricardo H. C. Takahashi

***Abstract*— This paper presents an algorithm for robust $\mathcal{H}_2/\mathcal{H}_\infty$ state-feedback control synthesis, with regional pole placement, based on a multiobjective optimization algorithm with non-smooth problem-solving capability. The problem is formulated with the state-feedback matrix coefficients as optimization parameters. The closed-loop performance obtained by means of the proposed strategy is assessed for the whole uncertainty-set through an LMI-based $\mathcal{H}_2$ and $\mathcal{H}_\infty$ guaranteed cost computation. The proposed strategy is compared with three former LMI approaches, for systems with polytope-bounded uncertainties, and presents better results.**

***Index Terms*— Robust $\mathcal{H}_2/\mathcal{H}_\infty$ control, regional pole placement, uncertain systems, multiobjective optimization.**

I. Introduction

Consider a LTI system described as

$$\left\{\begin{array}{rcl} \dot{x}(t) &=& Ax(t)+B_u u(t)+B_w w(t) \\ z_\infty(t) &=& C_{z1}x(t)+D_{zu1}u(t)+D_{zw1}w(t) \\ z_2(t) &=& C_{z2}x(t)+D_{zu2}u(t) \\ y(t) &=& C_y x(t) \end{array}\right. \quad (1)$$

where $x \in \mathbb{R}^n$ is the vector of state variables, $u \in \mathbb{R}^{p_u}$ is the vector of control inputs, $w \in \mathbb{R}^{p_w}$ is the vector of exogenous inputs (such as disturbance signals, sensor noise or reference signals), $z_\infty \in \mathbb{R}^{m_{z\infty}}$ is the vector of controlled variables related to the $\mathcal{H}_\infty$ performance, $z_2 \in \mathbb{R}^{m_{z2}}$ is the vector of controlled variables related to the $\mathcal{H}_2$ performance, and $y \in \mathbb{R}^{m_y}$ is the vector of measured outputs, with $C_y = I_n$.

Let T_∞ denote the closed-loop transfer function matrix from w to z_∞ and T_2 denote the closed-loop transfer function matrix from w to z_2. Our goal is to compute the state-feedback gain, K, that minimizes the $\mathcal{H}_\infty$ norm of T_∞, $||T_\infty||_\infty$, and the $\mathcal{H}_2$ norm of the T_2, $||T_2||_2$, and allocates the poles of the closed-loop system:

$$\dot{x}(t) = \underbrace{[A+B_u\,K]}_{A_{cl}}x(t)+B_w w(t) \quad (2)$$

$$z_\infty(t) = [C_{z1}+D_{zu1}K]x(t)+D_{zw1}w(t) \quad (3)$$

$$z_2(t) = [C_{z2}+D_{zu2}K]x(t) \quad (4)$$

E. N. Gonçalves is with Department of Electrical Engineering, Centro Federal de Educação Tecnológica de Minas Gerais, Av. Amazonas 7675, 31510-470, Belo Horizonte, MG, Brazil eduardong@des.cefetmg.br

R. M. Palhares is with Department of Electronics Engineering, Federal University of Minas Gerais, Av. Antônio Carlos 6627, 31270-010, Belo Horizonte, MG, Brazil palhares@cpdee.ufmg.br

R. H. C. Takahashi is with Department of Mathematics, Federal University of Minas Gerais, Av. Antônio Carlos 6627 - 31270-010, Belo Horizonte, MG, Brazil rtakahashi@ufmg.br

at regions $\mathcal{D}$ of the complex plane, where the matrices A, B_u, B_w, C_{z1}, D_{zu1}, D_{zw1}, C_{z2}, and D_{zu2} in (1) vary within a fixed polytope of matrices, i.e.,

$$\left[\begin{array}{ccc} A & B_u & B_w \\ C_{z1} & D_{zu1} & D_{zw1} \\ C_{z2} & D_{zu2} & 0 \end{array}\right] = \left\{\sum_{i=1}^{N}\alpha_i\left[\begin{array}{ccc} A_i & B_{u\,i} & B_{w\,i} \\ C_{z1\,i} & D_{zu1\,i} & D_{zw1\,i} \\ C_{z2\,i} & D_{zu2\,i} & 0 \end{array}\right] : \alpha_i \geq 0, \sum_{i=1}^{N}\alpha_i = 1\right\} \quad (5)$$

where N is the number of polytope vertices.

The paper [1] presented an important development in the state-feedback $\mathcal{H}_2/\mathcal{H}_\infty$ control synthesis with regional pole placement in a general class of convex subregions of the complex plane, with an Linear Matrix Inequality (LMI)-based formulation. A potential drawback of the formulation presented in that paper and other ones that employ the same approach, however, is that the Lyapunov matrix used to enforce system performance and the regional pole placement constraint is itself involved in the calculus of the state-feedback gain. This means that the only possible solutions for such design procedures are the ones that admit a single Lyapunov matrix for the whole uncertainty set and for the LMI formulation of all control objectives. Since these solutions are only a subset of all possibly relevant solutions, this constitute a source of conservatism in several LMI-based robust performance synthesis methodologies that is particularly important for systems with polytope-bounded uncertainty.

Several recent papers have proposed new LMI formulations aiming less conservative formulations through the use of multiple or parameter-dependent Lyapunov matrices. The paper [2] proposed an enhanced LMI characterization based on a reciprocal variant of the Projection Lemma, in addition to the classical linearizing transformations. That work dealt with a range of design objectives including the problem of exact assignment of the closed-loop eigenvalues to prescribed locations of the complex plane while enforcing Lyapunov-type constraints such as multi-channel $\mathcal{H}_2$ performance. This enhanced LMI characterization allow the use of different Lyapunov matrices for each vertex of the polytope (5) and each stability/performance specification. The paper [3] describes a dilated LMI characterization for continuous time robust multiobjective $\mathcal{H}_2/\mathcal{D}$-stability synthesis for polytope-uncertainty systems based on the use

of non-common parameter-dependent Lyapunov variables. The paper [4] extends the results in [3] to more enhanced dilated LMIs through the introduction of an adjustable arbitrary parameter. The paper [5] presented a new LMI-based robust $\mathcal{D}$-stability sufficient condition for the existence of parameter-dependent Lyapunov functions, which provides additional degrees of freedom supplied by the introduction of new matrix variables.

The present paper adopts another approach for solving the same problem: the synthesis problem is stated as a multiobjective problem, with objectives defined as the $\mathcal{H}_2$ and $\mathcal{H}_\infty$ norms in all polytope vertices and regional pole location constraints. Instead of building an LMI-based synthesis algorithm, a non-linear multiobjective algorithm for non-smooth optimization is employed [6], directly in the controller parameters. The robust attainment of the control objectives in the whole uncertainty polytope is guaranteed by LMI-based analysis tools borrowed from [7] and adapted from [1]. As shown by means of illustrative examples, the proposed strategy can compute the state-feedback gain satisfying the robust performance specifications and the pole placement constraints. The proposed strategy provides better $\mathcal{H}_2$ and $\mathcal{H}_\infty$ performance in comparison with LMI approaches, for all examples.

II. Problem Formulation

Let $A_{cl\,i}(K)$ denote the closed-loop matrix A_{cl} for polytope vertex i and for controller K. Let $\mathcal{D} \subset \mathbb{C}_-$ be a region in the complex plane, such as the ones defined in [1], to which the closed-loop poles must belong. Define the set Ω as:

$$\Omega \triangleq \{K \mid \lambda(A_{cl\,i}(K)) \in \mathcal{D} \ \forall\ i = 1, \ldots, N\} \tag{6}$$

Define $\|T_{2_i}(K)\|_2^2$ as the closed-loop $\mathcal{H}_2$ norm for controller K and vertex i, and $\|T_{\infty_i}(K)\|_\infty$ as the closed-loop $\mathcal{H}_\infty$ norm for controller K and vertex i. An objective vector $f(K)$ is defined as:

$$f(K) = \begin{bmatrix} \|T_{2_1}(K)\|_2 \\ \vdots \\ \|T_{2_N}(K)\|_2 \\ \|T_{\infty_1}(K)\|_\infty \\ \vdots \\ \|T_{\infty_N}(K)\|_\infty \end{bmatrix} \tag{7}$$

The set Ω^* is defined as:

$$\begin{array}{l} \Omega^* \triangleq \{K^* \in \Omega \mid \nexists K \in \Omega \text{ such that} \\ f(K) \leq f(K^*) \text{ and } f(K) \neq f(K^*)\} \end{array} \tag{8}$$

The vector comparison operators $\leq$ and $\neq$ have the usual meaning adopted in multiobjective optimization [8]: $x \leq\ y \Rightarrow x_i \leq y_i, \forall i$, and $x \neq\ y \Rightarrow \exists i \mid x_i \neq y_i$.

In order to approximate the solutions for the problem of synthesis of controllers that minimize (in a multiobjective sense) $||T_\infty||_\infty$ and $||T_2||_2$ for the whole uncertainty polytope while constraining the closed-loop poles in a specified region $\mathcal{D}$ of the complex plane, the auxiliary problem of finding controllers in the set Ω^* is employed here.

A. "Scalarization" Approach: The Hybrid Weighting and Constraint Problem - $P(\lambda, \epsilon)$

The strategy to obtain the non-dominated solutions relies in a transformation of the vector optimization problem in an equivalent scalar optimization problem that leads to a multiobjective solution. The "scalarization" method employed here combines the weighting and the constraint problem described in [8]. In the weighting problem, the objective is to minimize a weighted sum of the objective functions. In the ϵ-constraint problem, it is considered one objective function each time with the other objective functions treated as constraints.

Let $\Lambda = \{\lambda | \lambda \in \mathbb{R}^N, \lambda_i \geq 0$ and $\sum_{i=1}^N \lambda_i = 1\}$ be a set of nonnegative weights and γ an $\mathcal{H}_\infty$ norm upper bound specification. The non-dominated solutions of the multiobjective control problem (8) can be characterized in terms of the hybrid weighting and constraint problem $P(\lambda, \epsilon)$ [8]:

$$\left\{ \begin{array}{l} \min\limits_x \sum\limits_{i=1}^N \lambda_i f_i(x) \\ \quad \text{subject to:} \quad \begin{array}{l} f_{N+k}(x) \leq \epsilon_k, k = 1, \ldots, N \\ g_j(x) \leq 0, j = 1, \ldots, r \end{array} \end{array} \right. \tag{9}$$

where x is the parameter vector with the entries of the state-feedback gain vector, $f_i = \|T_{2_i}\|_2^2$, $i = 1, \ldots, N$, and $f_i = \|T_{\infty_i}\|_\infty^2$, $i = N+1, \ldots, 2N$, are the objective functions, $\epsilon_k = \gamma$, $k = 1, \ldots, N$, are the entries of the $\epsilon-$constraint vector, and $g_j(x)$, $j = 1, \ldots, r$, are the regional pole placement constraints.

The set of the non-dominated solutions of the problem (8) can be obtained by systematically varying the weighting vector $\lambda = [\lambda_1 \ldots \lambda_N] \in \Lambda$ and the γ constraint.

B. The Cone-Ellipsoid Algorithm

The scalar optimization problem (9) can be solved by the ellipsoid algorithm described by the recursive equations [6], [9]:

$$x_{k+1} = x_k - \beta_1 \frac{Q_k m_k}{(m_k^T Q_k m_k)^{\frac{1}{2}}} \tag{10}$$

$$Q_{k+1} = \beta_2 \left(\ Q_k - \frac{\beta_3 (Q_k m_k)(Q_k m_k)^T}{m_k^T Q_k m_k} \ \right) \tag{11}$$

with

$$\beta_1 = \tfrac{1}{n+1} \quad \beta_2 = \tfrac{n^2}{n^2-1} \quad \beta_3 = 2\beta_1 \tag{12}$$

where $x \in \mathbb{R}^d$ is the optimization parameter vector. Let $f(x) : \mathbb{R}^d \to \mathbb{R}$ be the objective function and $g(x) : \mathbb{R}^d \to \mathbb{R}^r$ be the constraint vector. In the conventional ellipsoid method, the vector m_k is calculated as the gradient (or sub-gradient) of the most violated constraint when x_k is not a feasible solution, or as the gradient (or sub-gradient) of the objective function when x_k is a feasible solution. In this

work, the vector m_k will be calculated based on the cone-ellipsoid algorithm (CEA) proposed by [6]. In this method, when x_k is not feasible, the vector m_k is chosen as the normalized vector $m_k = m/\|m\|$ calculated as the sum of the gradients (or sub-gradients) of the active constraints:

$$m = \begin{cases} \nabla f(x) & \text{if} \quad g_j(x) < 0,\ \forall j = 1, \ldots, r \\ \sum_{j=1}^{r} s_j(x) & \text{if} \quad \exists j \mid g_j(x) \geq 0 \end{cases} \tag{13}$$

with

$$s_j(x) = \begin{cases} 0 & \text{if} \quad g_j(x) < 0 \\ \nabla g_j(x) & \text{if} \quad g_j(x) \geq 0 \end{cases} \tag{14}$$

where $\nabla(.)$ means the function gradient (or sub-gradient). The global convergence property that is valid for the ellipsoid algorithm in the case of convex non-smooth problems is inherited by CEA, with much faster convergence [6].

C. Guaranteed Cost Computation and Pole Placement Constraints

The multiobjective control problem defined by (8) is not a convex problem as in the case of the conventional LMI approach, and there is no guarantee that the $\mathcal{H}_2$ and $\mathcal{H}_\infty$ norms in the interior of the polytope defined by (5) will not be greater than the results obtained for the vertices of the polytope. Due to this, a $\mathcal{H}_2$ and $\mathcal{H}_\infty$ guaranteed cost computation must be performed, in order to assure the closed-loop robustness. The $\mathcal{H}_2$ guaranteed cost, δ_c, and the $\mathcal{H}_\infty$ guaranteed cost, γ_c, proposed in [7], are used in this work.

In the same way, the closed-loop pole placement constraints must be robustly verified via a "guaranteed" criterion that holds for the whole polytope. This is performed via a direct adaptation of the results presented in [1].

III. Illustrative Examples

Example 1 - Satellite

The system is a satellite consisting of two rigid bodies (main module and sensor module) connected by an elastic link (the "boom") [10], [11], [3]. The boom is modeled as a spring with torque constant k and viscous damping f that have uncertainty ranges:

$$0.09 \leq k \leq 0.4 \quad \text{and} \quad 0.0038 \leq f \leq 0.04$$

The state-space description for the satellite system is

$$\begin{bmatrix} \dot{\theta}_1 \\ \dot{\theta}_2 \\ \ddot{\theta}_1 \\ \ddot{\theta}_2 \end{bmatrix} = \begin{bmatrix} 0 & 0 & 1 & 0 \\ 0 & 0 & 0 & 1 \\ -\frac{k}{J_1} & \frac{k}{J_1} & -\frac{f}{J_1} & \frac{f}{J_1} \\ \frac{k}{J_2} & -\frac{k}{J_2} & \frac{f}{J_2} & -\frac{f}{J_2} \end{bmatrix} \begin{bmatrix} \theta_1 \\ \theta_2 \\ \dot{\theta}_1 \\ \dot{\theta}_2 \end{bmatrix} + \begin{bmatrix} 0 \\ 0 \\ \frac{1}{J_1} \\ 0 \end{bmatrix} u + \begin{bmatrix} 0 \\ 0 \\ \frac{1}{J_1} \\ 0 \end{bmatrix} w \tag{15}$$

$$z_\infty = \begin{bmatrix} 0 & 1 & 0 & 0 \end{bmatrix} \begin{bmatrix} \theta_1 \\ \theta_2 \\ \dot{\theta}_1 \\ \dot{\theta}_2 \end{bmatrix} \tag{16}$$

$$z_2 = \begin{bmatrix} 1 & 0 & 0 & 0 \\ 0 & 1 & 0 & 0 \\ 0 & 0 & 0 & 0 \end{bmatrix} \begin{bmatrix} \theta_1 \\ \theta_2 \\ \dot{\theta}_1 \\ \dot{\theta}_2 \end{bmatrix} + \begin{bmatrix} 0 \\ 0 \\ 1 \end{bmatrix} u \tag{17}$$

where θ_1 and θ_2 are the yaw angles for the main body and the sensor module, u is the control torque, and w is a torque disturbance on the main body. It is considered that $J_1 = 1$ and $J_2 = 1$.

Firstly, it is considered the $\mathcal{H}_2$ control synthesis problem that does not include the $\mathcal{H}_\infty$ norm constraints in the optimization problem (9). The goal is to design a robust state-feedback controller that minimizes the $||T_2||_2$ norm and places the closed-loop eigenvalues in the intersection of the half-plane region $Real(\lambda(A_{cl})) \leq -0.1$, the disk region $|\lambda(A_{cl}) - 2.51| \leq 2.5$, and the cone sector centered at the origin $\angle\lambda(A_{cl}) \geq 2\pi/3$, for all possible values of the parameters k and f. The displacement of the disk region is a requirement of the dilated LMI characterization [3] and the enhanced dilated LMI characterization [4], and are adopted in order to allow the comparison.

Table I presents the $\|T_2\|_2$ norms in the four vertices for different design strategies. The first three state-feedback gains in Table I were respectively obtained based on the conventional LMI approach [12], denoted by K_c, the dilated LMI characterization [3], denoted by K_d, and the enhanced dilated LMI characterization [4], denoted by K_e. The state-feedback gains denoted by $K_{\lambda i}$, $i = 1, \ldots, 5$, were computed by means of the problem (9) with the fixed initial values $x_0 = [1\ 1\ 1\ 1]$ and $Q_0 = 10^6 I_4$, and the following parameters: $\lambda_1 = [0.25\ 0.25\ 0.25\ 0.25]$, $\lambda_2 = [0.7\ 0.1\ 0.1\ 0.1]$, $\lambda_3 = [0.1\ 0.7\ 0.1\ 0.1]$, $\lambda_4 = [0.1\ 0.1\ 0.7\ 0.1]$, and $\lambda_5 = [0.1\ 0.1\ 0.1\ 0.7]$. The state-feedback gains to which Table I makes reference are:

$$\begin{aligned} K_c &= [-8.6004 \quad 4.9970 \quad -5.1103 \quad -20.6576] \\ K_d &= [-5.2577 \quad 3.3140 \quad -3.8221 \quad -9.0033] \\ K_e &= [-6.1817 \quad 3.6813 \quad -4.1145 \quad -12.9071] \\ K_{\lambda 1} &= [-2.5682 \quad 1.8415 \quad -2.6842 \quad -3.1983] \\ K_{\lambda 2} &= [-2.6923 \quad 1.6842 \quad -2.7653 \quad -3.5195] \\ K_{\lambda 3} &= [-2.7373 \quad 1.7923 \quad -2.7242 \quad -3.6129] \\ K_{\lambda 4} &= [-2.6189 \quad 1.7344 \quad -2.7415 \quad -3.3321] \\ K_{\lambda 5} &= [-2.6316 \quad 1.6412 \quad -2.8338 \quad -3.3240] \end{aligned}$$

The $\mathcal{H}_2$ guaranteed cost, δ_c, was calculated for each controller in Table I. The state-feedback gains $K_{\lambda i}$, computed by the multiobjective non-convex problem (8), provide better $\mathcal{H}_2$ guaranteed costs than the state-feedback gains computed by the LMI approaches. One can note that all

TABLE I

$\mathcal{H}_2$ NORMS FOR EACH VERTEX OF THE POLYTOPE AND THE $\mathcal{H}_2$ GUARANTEED COST, δ_c, FOR EXAMPLE 1. K_c: [12] DESIGN, K_d: [3] DESIGN, K_e: [4] DESIGN, $K_{\lambda i}$: THE PROPOSED DESIGN.

	$\|T_{2_1}\|_2$	$\|T_{2_2}\|_2$	$\|T_{2_3}\|_2$	$\|T_{2_4}\|_2$	δ_c
K_c	1.8570	1.8873	1.8684	1.8969	1.9265
K_d	1.6349	1.6547	1.6377	1.6563	1.7265
K_e	1.6950	1.7242	1.7020	1.7292	1.7796
$K_{\lambda 1}$	1.4482	1.4527	1.4404	1.4462	1.7091
$K_{\lambda 2}$	1.4390	1.4453	1.4324	1.4395	1.6921
$K_{\lambda 3}$	1.4406	1.4483	1.4341	1.4424	1.6804
$K_{\lambda 4}$	1.4413	1.4464	1.4341	1.4402	1.6983
$K_{\lambda 5}$	1.4445	1.4484	1.4374	1.4425	1.7124

LMI solutions are dominated by the proposed solutions in this case.

For the multiobjective $\mathcal{H}_2/\mathcal{H}_\infty$ control synthesis, the solutions obtained by the multiobjective problem (8) will be compared with the solutions calculated with the function `msfsyn` provided by the MATLAB® *LMI Control Toolbox* [10]. In this case, the goal is to design a robust state-feedback controller that minimizes the $\|T_2\|_2$ norms, achieves $\|T_\infty\|_\infty \leq 0.8$, and places the closed-loop eigenvalues into the intersection of the half-plane region $Real(\lambda(A_{cl})) \leq -0.1$, the disk region $|\lambda(A_{cl}) - 10.01| \leq 10$, and the cone sector centered at the origin $\angle\lambda(A_{cl}) \geq 2\pi/3$, for all possible values of the parameters k and f.

Table II presents the $\mathcal{H}_2$ norms, $\mathcal{H}_2$ guaranteed costs, $\mathcal{H}_\infty$ norms, and $\mathcal{H}_\infty$ guaranteed costs in the four vertices for the following state-feedback gains:

$$
\begin{aligned}
K_{c1} &= [-11.2990 \quad 7.2343 \quad -5.7931 \quad -25.6606] \\
K_{c2} &= [-12.7603 \quad 7.4562 \quad -6.1823 \quad -31.4735] \\
K_{c3} &= [-15.3984 \quad 7.6133 \quad -6.8306 \quad -42.4584] \\
K_{c4} &= [-21.4164 \quad 6.0715 \quad -8.1570 \quad -71.4057] \\
K_{\lambda 1} &= [-5.3050 \quad 2.4234 \quad -3.4892 - 10.6763] \\
K_{\lambda 2} &= [-6.2201 \quad 2.3859 \quad -3.8105 \quad -13.8705] \\
K_{\lambda 3} &= [-7.8520 \quad 2.0945 \quad -4.2238 \quad -19.9619] \\
K_{\lambda 4} &= [-11.4863 \quad -0.0239 \quad -5.0555 \quad -36.0397] \\
K_{\lambda 5} &= [-16.6379 \quad -6.4945 \quad -5.9959 \quad -63.5656]
\end{aligned}
$$

The state feedback gains K_{ci}, $i = 1, \ldots, 4$, were computed through the function `msfsyn` with the $\|T_\infty\| \leq \gamma$ constraint fixed as 0.8, 0.6, 0.4, and 0.2 respectively. The gains $K_{\lambda i}$, $i = 1, \ldots, 5$, were obtained by the proposed method, with the initial values $x_0 = [1\ 1\ 1\ 1]$ and $Q_0 = 10^6 I_4$, the weighting vector $\lambda = [1/4\ 1/4\ 1/4\ 1/4]$ and the $\mathcal{H}_\infty$ upper bound γ fixed as 0.4, 0.3, 0.2, 0.1, and 0.05 respectively.

Table II shows that all state feedback gains computed with the conventional LMI approach are dominated by solutions derived from the proposed methodology. Figure 1 shows the values of the $\mathcal{H}_2$ guaranteed cost, δ_c, versus the $\mathcal{H}_\infty$ guaranteed cost, γ_c, for the state-feedback gains listed in Table II. The dominance of the proposed methodology solutions becomes clear.

TABLE II

$\mathcal{H}_2$ NORMS, $\mathcal{H}_2$ GUARANTEED COSTS, $\mathcal{H}_\infty$ NORMS, AND $\mathcal{H}_\infty$ GUARANTEED COSTS FOR THE FOUR VERTICES OF EXAMPLE 1. K_{ci}: `msfsyn` CONTROLLERS. $K_{\lambda i}$: PROPOSED METHODOLOGY CONTROLLERS.

	$\|T_{2_1}\|_2$ $\|T_{\infty_1}\|_\infty$	$\|T_{2_2}\|_2$ $\|T_{\infty_2}\|_\infty$	$\|T_{2_3}\|_2$ $\|T_{\infty_3}\|_\infty$	$\|T_{2_4}\|_2$ $\|T_{\infty_4}\|_\infty$	δ_c γ_c
K_{c1}	1.9794 0.2465	2.0067 0.2459	1.9919 0.2463	2.0178 0.2463	2.0409 0.3820
K_{c2}	2.0422 0.1892	2.0720 0.1884	2.0573 0.1890	2.0856 0.1884	2.1051 0.2954
K_{c3}	2.1432 0.1293	2.1763 0.1284	2.1625 0.1292	2.1939 0.1285	2.2103 0.2035
K_{c4}	2.3351 0.0660	2.3735 0.0652	2.3628 0.0659	2.3992 0.0652	2.4140 0.1054
$K_{\lambda 1}$	1.6061 0.3999	1.6426 0.3465	1.6123 0.3889	1.6460 0.3465	1.7164 0.6894
$K_{\lambda 2}$	1.6700 0.3000	1.7119 0.2610	1.6796 0.2913	1.7182 0.2613	1.7730 0.5240
$K_{\lambda 3}$	1.7632 0.1999	1.8149 0.1737	1.7781 0.1936	1.8258 0.1734	1.8684 0.3532
$K_{\lambda 4}$	1.9345 0.1000	2.0012 0.0868	1.9597 0.0962	2.0212 0.0868	2.0575 0.1814
$K_{\lambda 5}$	2.1178 0.0500	2.2002 0.0432	2.1561 0.0477	2.2316 0.0432	2.2711 0.0940

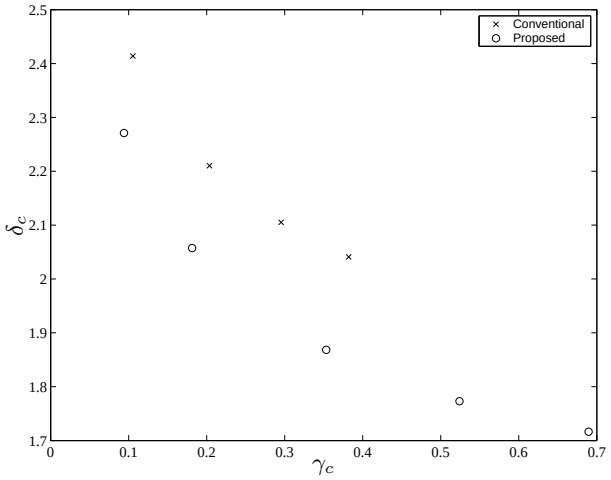

Fig. 1. $\mathcal{H}_2$ guaranteed cost, δ_c, versus the $\mathcal{H}_\infty$ guaranteed cost, γ_c, for the example 1

Example 2: A Quarter-car Active Vehicle Suspension

The quarter-car active suspension system model consists of the sprung mass m_1, the unsprung mass m_2, the tire linear spring with stiffness k_t, the suspension passive spring k, the suspension damper c, and, in parallel, an active device that controls the force u [13], [14]. The model has a vertical velocity w imposed by the road as exogenous input. The states variables for this system are: the suspension deflection, x_1; the tire deflection, x_2; the sprung mass velocity, x_3; the unsprung mass velocity, x_4; and an additional state variable representing the output of an integrator, x_5, with $\dot{x}_5 = x_1$. The state-space description for the active

TABLE III

$\mathcal{H}_2$ NORMS OF THE TWO VERTICES AND THE $\mathcal{H}_2$ GUARANTEED COST FOR EXAMPLE 2. K_c: [12] DESIGN, K_d: [3] DESIGN, K_e: [4] DESIGN, $K_{\lambda i}$: THE PROPOSED DESIGN.

	$\|T_{2_1}\|_2$	$\|T_{2_2}\|_2$	δ_c
K_c	20.7731	19.9337	22.8529
K_d	21.3034	20.4495	23.1619
K_e	20.8114	20.0107	22.5171
$K_{\lambda 1}$	12.7898	12.6919	14.4017
$K_{\lambda 2}$	12.7931	12.6904	14.4024
$K_{\lambda 3}$	12.7895	12.6934	14.4025

suspension is

$$\dot{x} = \begin{bmatrix} 0 & 0 & -1 & 1 & 0 \\ 0 & 0 & 0 & -1 & 0 \\ \frac{k}{m_1} & 0 & -\frac{c}{m_1} & \frac{c}{m_1} & 0 \\ -\frac{k}{m_2} & \frac{k_t}{m_2} & \frac{c}{m_2} & -\frac{c}{m_2} & 0 \\ 1 & 0 & 0 & 0 & 0 \end{bmatrix} x + \begin{bmatrix} 0 \\ 0 \\ \frac{1}{m_1} \\ -\frac{1}{m_2} \\ 0 \end{bmatrix} u + \begin{bmatrix} 0 \\ 1 \\ 0 \\ 0 \\ 0 \end{bmatrix} w$$

$$z_\infty = \begin{bmatrix} 1 & 0 & 0 & 0 & 0 \end{bmatrix} x$$

$$z_2 = \begin{bmatrix} 1 & 0 & 0 & 0 & 0 \\ 0 & 0 & 1 & 0 & 0 \\ 0 & 0 & 0 & 0 & 0 \end{bmatrix} x + \begin{bmatrix} 0 \\ 0 \\ 0.001 \end{bmatrix} u$$

where $231.12\text{Kg} \leq m_1 \leq 346.68\text{Kg}$, $m_2 = 28.58\text{Kg}$, $k = 10.000\text{N/m}$, $k_t = 155.900\text{N/m}$, and $c = 850\text{Ns/m}$.

In this case the uncertain system is represented by a polytope with two vertices derived from the extreme limits of m_1. The pole placement constraints are defined as the intersection of the half-plane region $Real(\lambda(A_{cl_i})) \leq -3$ and the disk region $|\lambda(A_{cl_i}) - 35.1| \leq 35$.

Table III presents the $\mathcal{H}_2$ norms of the two vertices achieved by several designs using the same nomenclature of the example 1.

The state feedback gains listed in Table III are:

$$\begin{aligned} K_c &= [0.185 \quad 9.325 \quad -0.096 \quad 0.124 \quad 3.140] \times 10^4 \\ K_d &= [-0.129 \quad 9.740 \quad -0.051 \quad 0.112 \quad 1.844] \times 10^4 \\ K_e &= [-0.166 \quad 9.601 \quad -0.046 \quad 0.111 \quad 1.706] \times 10^4 \\ K_{\lambda 1} &= [0.242 \quad 0.328 \quad -0.052 \quad 0.019 \quad 1.171] \times 10^5 \\ K_{\lambda 2} &= [0.239 \quad 0.326 \quad -0.052 \quad 0.019 \quad 1.103] \times 10^5 \\ K_{\lambda 3} &= [0.243 \quad 0.329 \quad -0.052 \quad 0.019 \quad 1.191] \times 10^5 \end{aligned}$$

The state-feedback gains $K_{\lambda i}$ were obtained with the optimization problem 9 with $x_0 = [100\ 100\ 100\ 100\ 100]^T$, $Q_0 = 10^{10} I_5$, and the weighting vectors: λ_1 = [0.5 0.5], λ_2 = [0.1 0.9], and λ_3 = [0.9 0.1]. In this case, the resulting gains become very similar, in spite of variation of the weighting vector λ, possibly indicating the occurrence of an isolated optimum in the Pareto-set of the problem. One can note that the proposed strategy provides better $\mathcal{H}_2$ guaranteed costs in this case too.

TABLE IV

$\mathcal{H}_2$ NORMS, $\mathcal{H}_2$ GUARANTEED COSTS, $\mathcal{H}_\infty$ NORMS, AND $\mathcal{H}_\infty$ GUARANTEED COSTS OF THE TWO VERTICES FOR THE EXAMPLE 2. K_{ci}: `msfsyn` CONTROLLERS. $K_{\lambda i}$: PROPOSED METHODOLOGY CONTROLLERS.

	$\|T_{2_1}\|_2$ $\|T_{\infty_1}\|_\infty$	$\|T_{2_2}\|_2$ $\|T_{\infty_2}\|_\infty$	δ_c γ_c
K_{c1}	27.34 0.286	25.78 0.357	29.52 0.411
K_{c2}	27.00 0.244	25.45 0.305	29.27 0.354
K_{c3}	26.57 0.203	25.06 0.255	28.92 0.298
K_{c4}	26.00 0.156	24.53 0.199	28.46 0.234
$K_{\lambda 1}$	21.64 0.343	20.77 0.354	23.02 0.426
$K_{\lambda 2}$	21.64 0.339	20.77 0.351	23.02 0.423
$K_{\lambda 3}$	21.64 0.345	20.77 0.355	23.01 0.428
$K_{\lambda 4}$	21.72 0.289	20.83 0.300	23.10 0.365
$K_{\lambda 5}$	22.06 0.189	21.09 0.200	23.54 0.248

For the multiobjective $\mathcal{H}_2/\mathcal{H}_\infty$ control synthesis, the $\mathcal{H}_\infty$ norm constraints $\|T_{\infty_i}\|_\infty \leq 0.8$, $i = 1, \ldots, 2$ are included. Table IV presents the $\mathcal{H}_2$ and $\mathcal{H}_\infty$ norms for the two vertices achieved by the following state-feedback gains:

$$\begin{aligned} K_{c1} &= [-0.502 \quad 11.716 \quad -0.001 \quad 0.082 \quad 1.061] \times 10^4 \\ K_{c2} &= [-0.444 \quad 11.590 \quad -0.008 \quad 0.086 \quad 1.214] \times 10^4 \\ K_{c3} &= [-0.359 \quad 11.423 \quad -0.018 \quad 0.090 \quad 1.440] \times 10^4 \\ K_{c4} &= [-0.218 \quad 11.192 \quad -0.034 \quad 0.097 \quad 1.828] \times 10^4 \\ K_{\lambda 1} &= [-0.778 \quad 10.009 \quad -0.037 \quad 0.111 \quad 0.125] \times 10^4 \\ K_{\lambda 2} &= [-0.777 \quad 9.992 \quad -0.038 \quad 0.111 \quad 0.121] \times 10^4 \\ K_{\lambda 3} &= [-0.777 \quad 9.990 \quad -0.038 \quad 0.111 \quad 0.119] \times 10^4 \\ K_{\lambda 4} &= [-0.777 \quad 9.991 \quad -0.038 \quad 0.111 \quad 0.122] \times 10^4 \\ K_{\lambda 5} &= [-0.776 \quad 9.993 \quad -0.039 \quad 0.111 \quad 0.118] \times 10^4 \end{aligned}$$

The state feedback gains K_{ci}, $i = 1, \ldots, 4$, were computed through the function `msfsyn` with the $\mathcal{H}_\infty$ upper bound γ fixed as 0.7, 0.6, 0.5, and 0.4, respectively. The state-feedback gains $K_{\lambda i}$, $i = 1, \ldots, 4$, were obtained based on the optimization problem (9) with $x_0 = [100\ 100\ 100\ 100\ 100]^T$, $Q_0 = 10^{10} I_5$, the weighting vector $\lambda = [0.5\ 0.5]$, and the $\mathcal{H}_\infty$ upper bound γ fixed as 0.6, 0.5, 0.4, 0.3, and 0.2, respectively. One can note in Table IV that, comparing gains with similar $\mathcal{H}_\infty$ guaranteed cost values, the proposed strategy achieved better $\mathcal{H}_2$ guaranteed costs than the conventional LMI approach.

Figure 2 shows the $\mathcal{H}_2$ and $\mathcal{H}_\infty$ norms for the feasible solutions versus the iteration number in the computing of the state feedback gain $K_{\lambda 1}$. The algorithm converged in 445 iterations. Figure 3 shows the optimization parameters x_i, $i = 1, \ldots, 5$, versus the iteration number in the computation of controller $K_{\lambda 1}$. Figure 4 shows the fulfillment of the pole location constraints for several values of m_1 in the specified range, for controller $K_{\lambda 1}$.

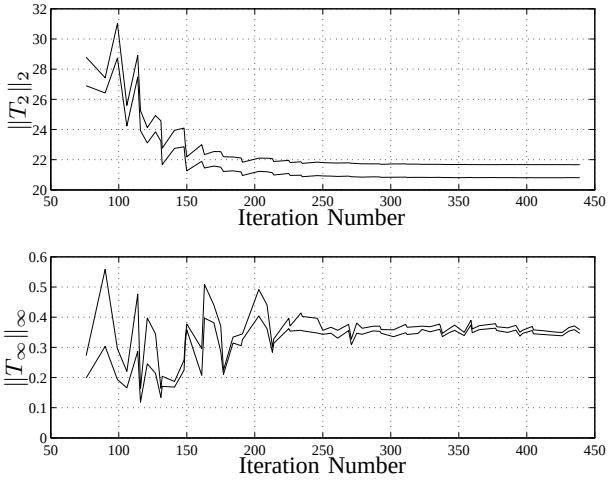

Fig. 2. $\mathcal{H}_2$ and $\mathcal{H}_\infty$ norms for the feasible solutions versus the iteration number in the computation of the state feedback gain $K_{\lambda 1}$

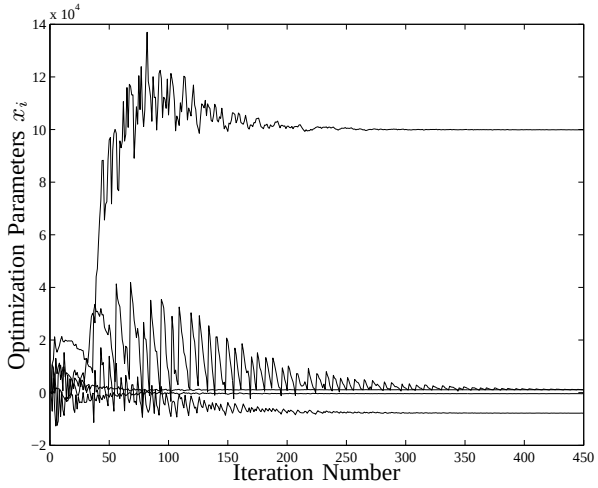

Fig. 3. The optimization parameters x_i, $i = 1, \ldots, 5$, versus the iteration number in the computation of the controller $K_{\lambda 1}$

IV. Conclusions

In this paper, a strategy for robust multiobjective $\mathcal{H}_2/\mathcal{H}_\infty$ control design with regional pole placement for systems with polytope-bounded uncertainty was presented. The proposed strategy relies on an efficient algorithm for non-smooth optimization, applied to the multiobjective problem of $\mathcal{H}_2$ and $\mathcal{H}_\infty$ norms minimization over the set of polytope vertices. The control synthesis, performed directly in the space of controller parameters, avoids the conservatism that appears in LMI-based approaches. LMI-based guaranteed costs computations guarantee the resulting controllers validity in the whole polytope.

Considering the analyzed examples, the proposed strategy presented better results than LMI-synthesis approaches.

The proposed approach can be applied, without substantial modification, to the cases of: discrete-time systems, static output feedback, decentralized control, fixed-order dynamic output feedback, etc, with polytope-bounded uncertainty in all cases.

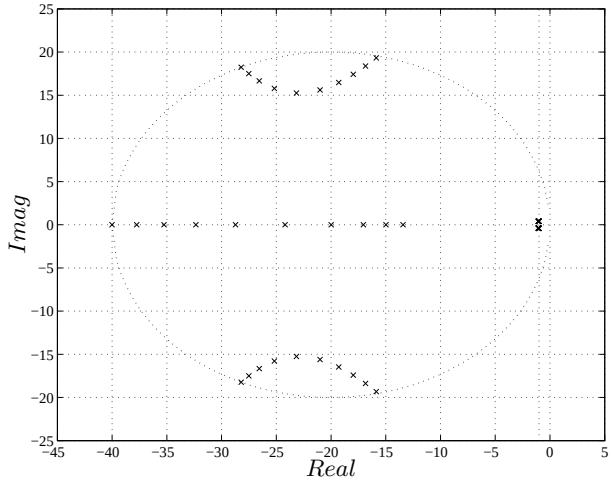

Fig. 4. Closed-loop pole locations for controller $K_{\lambda 1}$ with m_1 in the specified range.

References

[1] M. Chilali and P. Gahinet, "$\mathcal{H}_\infty$ design with pole placement constraints: An LMI approach," *IEEE Transactions on Automatic Control*, vol. 41, no. 3, pp. 358–367, 1996.

[2] P. Apkarian, H. D. Tuan, and J. Bernussou, "Continuous-time analysis, eigenstructure assignment and $\mathcal{H}_2$ synthesis with enhanced LMI characterizations," *IEEE Transactions on Automatic Control*, vol. 46, no. 12, pp. 1941–1946, 2001.

[3] Y. Ebihara and T. Hagiwara, "New dilated LMI characterizations for continuous-time control design and robust multiobjective control," *Proceedings of the American Control Conference*, pp. 47–52, 2002.

[4] ——, "Robust controller synthesis with parameter-dependent lyapunov variables: A dilated LMI approach," *Proceedings of the 41st IEEE Conference on Decision and Control*, pp. 4179–4184, 2002.

[5] D. Peaucelle, D. Arzelier, O. Bachelier, and J. Bernussou, "A new robust $\mathcal{D}$-stability condition for real convex polytopic uncertainty," *Systems & Control Letters*, vol. 40, pp. 21–30, 2000.

[6] R. H. C. Takahashi, R. R. Saldanha, W. Dias-Filho, and J. A. Ramírez, "A new constrained ellipsoidal algorithm for nonlinear optimization with equality constraints," *IEEE Transactions on Magnetics*, vol. 39, no. 3, pp. 1289–1292, 2003.

[7] R. M. Palhares, R. H. C. Takahashi, and P. L. D. Peres, "$\mathcal{H}_2$ and $\mathcal{H}_\infty$ guaranteed costs computation for uncertain linear systems," *International Journal of Systems Science*, pp. 183–188, 1997.

[8] V. Chankong and Y. Y. Haimes, *Multiobjective Decision Making: Theory and Methodology*, North-Holland, Ed. New York: Elsevier, 1983.

[9] S. Kanev, B. de Schutter, and M. Verhaegen, "An ellipsoidal algorithm for probabilistic robust controller design," *System & Control Letters*, vol. 49, pp. 365–375, 2003.

[10] P. Gahinet, A. Nemirovski, A. J. Laub, and M. Chilali, *LMI Control Toolbox: For Use with MATLAB®*, The MATH WORKS Inc., Natick, 1995.

[11] Y. Ebihara, T. Hagiwara, and T. Shimomura, "Multiobjective state-feedback control design with non-common LMI solutions: Change of variables via affine functions," *Proceedings of the American Control Conference*, pp. 848–853, 2001.

[12] C. Scherer, P. Gahinet, and M. Chilali, "Multiobjective output-feedback control via LMI optimization," *IEEE Transactions on Automatic Control*, vol. 42, no. 7, pp. 896–911, 1997.

[13] M. M. ElMadany and M. I. AL-Majed, "Quadratic synthesis of active controls for a quarter-car model," *Journal of Vibration and Control*, vol. 7, pp. 1237–1252, 2001.

[14] V. J. S. Leite and P. L. D. Peres, "Robust pole location for an active suspension quarter-car model through parameter dependent control," *Proceedings of the 2002 International Conference on Control Applications*, vol. 18, no. 20, pp. 447–452, 2002.